

## NUMERICAL AND EXPERIMENTAL HEAT AND MASS TRANSFER ANALYSIS DURING OKARA DRYING

**Camila Augusto Perussello, camila\_ea@yahoo.com.br**  
**Viviana Cocco Mariani, viviana.mariani@pucpr.br**  
**Álvaro César Camargo do Amarante, alvaro.amarante@pucpr.br**  
Mechanical Engineering Department  
Pontifical Catholic University of Paraná  
Rua Imaculada Conceição, 1155, Zip Code 80215-901, Curitiba - PR - Brasil

**Abstract.** *This work analyzes experimental and numerically the conjugated mass and heat transfer during the drying of the residue obtained in the soy hydrosoluble extract production (okara). This drying process consists in submitting the extruded okara on the shape of pellets to a fixed bed dryer until they achieve the equilibrium humidity. The process parameters, time and temperature, are correlated to the darkening level of the final product. The temperatures tested are 170°C, 150°C and 130°C. The moisture and temperature profiles at the pellets were measured experimentally for each simulated process and the level of the product darkening was evaluated visually. The best process temperature, in terms of darkening level, is the one that uses 130°C. The process which uses 150°C lasts only one minute more than the lowest temperature, however it causes an undesirable color at the pellets. The pellets dried at 170°C present an exaggerated brown color. For the numerical analysis the drying governing equations, the Fourier's Law and the Fick's Law, were solved by the Implicit Finite Difference Method. All the thermal properties of the okara utilized at the simulation, density, density of the solid fraction, specific heat, thermal conductivity, thermal diffusivity, mass diffusivity, heat transfer coefficient and mass transfer coefficient were obtained by literature equations which utilize data obtained at laboratory, and the latent heat for the water vaporization and water vapor specific heat were obtained in literature. In order to calculate these properties, the porosity, which was obtained by the picnometry method, was considered inside the pellets. The processes were simulated numerically using Matlab. The results showed an adequate efficiency of the proposed drying method and a good agreement between experimental and numerical results were obtained ( $R^2 > 0.99$ ).*

**Keywords:** *Drying, Numerical Analysis, Heat Transfer, Mass Transfer, Thermal Properties, Okara.*

### 1. INTRODUCTION

Okara is the residue obtained during the extraction of the soy hydrosoluble extract, that is, it is the soy beverage and tofu production residue. Considering that the extraction process involves the soy grain humid milling, the solid residue obtained is a mass with around 75% humidity, containing approximately 95% of the soy grain solid components. This indicates that the residue nutritional value is very high and that large quantities of residue are obtained during the extract fabrication process (Smith and Circle, 1983). Another okara characteristic is the fast deterioration: on about 8 hours the product ferments and turns on improper for consuming. The solution for avoiding the high expenses with effluent treatment (because of the large volume of okara produced and discarded) is submitting okara to a drying process, which will preserve its integrity by decreasing its water activity, allowing its use in other foods.

Drying operations are very important in the food industry processes. Because of the changes on its chemical, physical and biological characteristics, products submitted to drying have higher conservation, because of the degradation reactions decreasing, have its volume reduced, facilitating transport and storing, and can have its flavor and color modified. However, depending on the intensity and on the effect of the drying process, the loss or inutility of the product for a certain function can occur. Thus, the drying parameters (like air temperature, velocity and relative humidity) on the final product quality must be studied. The drying process proposed in this work consists in submitting the extruded okara pellets to a drying process using a fixed bed dryer until they achieve the equilibrium humidity content. Some works about okara drying are found at literature, but they approach only the drying processes at jet bed dryers or by the eletrohydrodynamic technique.

Wachiraphansakul e Devahastin (2005) investigated the okara drying using a jet bed dryer with sorbent particles. They concluded that the addition of inert particles improves the drying kinetics and the dried product quality. Lescano et al. (2005) analyzed the okara drying by the same technique. They studied the influence of okara and inert material quantities on process time and concluded that the inert material, at the quantities used, did not have influence on drying time. Tatsumi et al. (2006) studied the eletrohydrodynamic technique (EHD) effect on the okara drying. In comparison to a control sample, which was dried by convection in a stove at 105°C, the drying time using the EHD technique was reduced in 15 to 40% for obtaining a product with 10% humidity wet basis, however the sample presented a more intense brown color. Taruna and Jindal (2002) investigated the okara drying in a moving bed of inert particles submitted to a vortex movement. They concluded that inlet air temperature had influence on the exit air relative humidity and on its temperature, that a larger alimentation rate of okara or inert material increased the water

evaporation specific rate and reduced the process energy. Also studying the okara drying on a jet bed dryer, Coronel and Tobinaga (2004) concluded that the better drying condition, in terms of final product humidity and color, were low temperatures ( $\approx 75^{\circ}\text{C}$ ) and retention time of around 10.5 minutes, while the use of temperatures larger than  $80^{\circ}\text{C}$  with retention time larger than 6 minutes is prejudicial to okara powder humidity and to its oil absorption capacity. Lescano et al. (2005b) characterized physically the dried and humid okara and the inert material used at okara jet bed drying, determining properties like granulometry, apparent, volumetric and real densities and porosity. Lescano et al. (2006) determined either the water apparent diffusivity in okara ( $D_{ap}$ ) from drying experimental data of okara jet bed drying, using the 6 first terms of the Fick's model serial solution. Drying experiments were made varying the inlet air temperature (50 to  $70^{\circ}\text{C}$ ), material grinding time (50 to  $70^{\circ}\text{C}$ ) and the ratio between inlet air flow and inert material jet, and the more significative variables for  $D_{ap}$  were inlet air temperature and okara particles grinding time. Values obtained for  $D_{ap}$  placed between  $2,439 \times 10^{-9}$  and  $10,519 \times 10^{-9} \text{ m}^2/\text{s}$ .

In this work, besides the drying experimental tests, which showed humidity and temperature variation inside the pellets, the okara thermal properties were determined from the product centesimal composition using literature equations, the problem numerical analysis was made using the implicit finite difference method, numerical and experimental results were compared and the better drying condition, which permits obtaining dehydrated okara pellets with the lightest color possible, was obtained.

## 2. MATERIAL AND METHODS

The drying method proposed in this work uses okara on the shape of 5 mm pellets, which are dried in a fixed bed dryer. In the pellets the heat and mass transfer is easier, promoting a faster drying, thus causing less darkening to the product.

### 2.1 Drying tests

In order to promote the drying tests, a spray-dryer adaptation was made to simulate the fixed bed dryer. The spray-dryer is an equipment that dries liquid products through its aspersion on the shape of very small drops in a hot air current. This way, the product leaves the process on the form of powder with reduced humidity content. For simulating a fixed bed, a tube with 12 cm diameter that fits on the air exit was built. At the end of the tube a structure which consists on a 5 cm height cylinder was encased. This structure has its upper part opened to permit the air flow and its lower part is a drilled net, which accommodates the product that is being dried, as Fig. 1 shows.



Figure 1 – Lab-Plant Spray-dryer, model SD-05.

The drying tests (all of them in triplicate) were accomplished with three temperatures,  $130^{\circ}\text{C}$ ,  $150^{\circ}\text{C}$  and  $170^{\circ}\text{C}$ . The air supplied by the spray-dryer has its relative humidity and velocity variable with temperature. Relative humidity was experimentally obtained through the air wet bulb and the dry bulb temperature measurements. The dry bulb temperature was measured with a thermometer, while the wet bulb temperature was measured with a thermometer with its extremity covered by a humid gauze. A psychometric chart was used to obtain the air relative humidity values, which are 1.17% for  $T = 130^{\circ}\text{C}$ , 0.77% for  $T = 150^{\circ}\text{C}$  and 0.38% for  $T = 170^{\circ}\text{C}$ . The air velocity was measured with a hot wire anemometer and the results are 0.044 m/s for  $T=130^{\circ}\text{C}$ , 0.051 m/s for  $T=150^{\circ}\text{C}$  and 0.073 m/s for  $T=170^{\circ}\text{C}$ .

The humidity analysis was made by the gravimetric method, which consists in submitting the sample to a convection drying in a stove at  $105^{\circ}\text{C}$  for around 8 hours, time sufficient to the water loss ceasing. Temperature profiles were obtained through the pellets temperature measurement with type T thermocouples. A data acquisition central (HP Agilent) and a computer were also used for data storage. Fig 2a shows the humidity versus time curves for each drying temperature used. It can be observed that higher process temperatures reduce drying times, which were 9 minutes, 10 minutes and 15 minutes for  $170^{\circ}\text{C}$ ,  $150^{\circ}\text{C}$  and  $130^{\circ}\text{C}$ , respectively. It can be seen that the curves referent to the drying

process using 150 and 170°C do not differ much, excepting the final part of the process. Until 4 minutes of drying, the curves behavior is very similar, however the process with the higher temperature reduces faster the product humidity after the fourth minute because the air relative humidity is lower (0.77% versus 1.17%) and the air velocity is higher (0.073 m/s versus 0.051 m/s). In despite of the differences on drying times, all the curves present the same tendency, that is, the humidity decreases rapidly until 5 minutes of process and after this the drying speed decreases. The humidity transfer velocity decreases because as the water content to be removed reduces, the remanent water in the product has to migrate to its surface and also because the water is stronger attached to the other food components, being more difficult to be removed.

Temperature profiles, which were measured at the center of the pellets for each different process temperature, can be seen at Fig. 2b. It can be observed that the kinetic curves present the same tendency: at the first minute temperature increases very fast and later the temperature increasing becomes slower and it stabilizes around 9 minutes of drying.

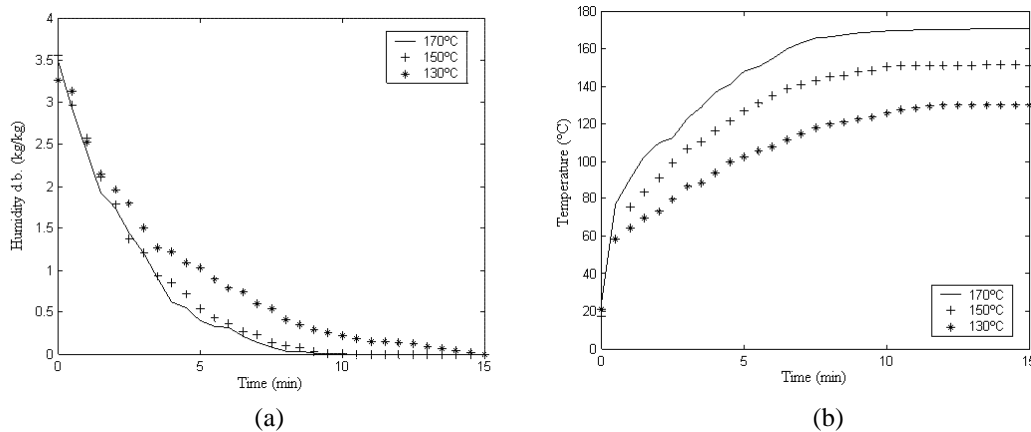


Figure 2 – (a) Okara pellets humidity versus drying time; (b) Okara pellets temperature versus drying time.

## 2.2 Thermal properties

The acquirement of a product thermal properties values during a drying process is essential to predict temperature distribution inside it and the humidity removal to the drying air. During drying, the food water content (and then, its centesimal composition), temperature and density vary considerably at each time interval resulting in variable thermal and mass diffusivity. As each process condition (time and temperature) influences directly on the product water loss during drying, all thermal properties were evaluated for each drying temperature used.

The okara thermal properties obtained from its drying were: density, specific heat, thermal conductivity, heat transfer coefficient, thermal diffusivity, mass diffusivity and mass transfer coefficient. All of them were obtained by literature equations that use product centesimal composition.

Firstly, the okara centesimal composition was analyzed at laboratory as according to standard techniques, which can be found in Matissek et al, 1998. In wet basis, the analysis gave the results (water = 76.49%, carbohydrates = 13.30%, fats = 0.58%, proteins = 9.15% and ashes = 0.48%), and in dry basis the results (carbohydrates = 56.57%, fats = 2.47%, proteins = 38.93% and ashes = 2.03%). The dry basis composition calculus from the wet basis composition is made by % Component =  $(x_n/x_s) \times 100$ , where  $x_n$  is the solid component percentage on the wet basis composition and  $x_s$  is the percentage of the whole solid fraction on the wet basis composition.

The product porosity,  $\epsilon$ , were also measured in order to calculate the okara centesimal composition including the air inside the pellets. Porosity is an important property that influences on food thermal properties. Its effect on specific heat is negligible, but its effect on density and thermal conductivity is important (Mannapperuma and Singh, 1988). Porosity was obtained at laboratory by the picnometry method and the experiment, made in triplicate, gave as result 23.68%. Density and thermal conductivity were obtained from the centesimal composition considering the porosity. Density is multiplied by a factor  $(1-\epsilon)$  to account the porosity effect. This adjust on density corrects also the thermal conductivity, which is calculated using density itself. In order to obtain density, specific heat and thermal conductivity, the properties of each okara pure component (water, carbohydrates, fats, proteins and ashes) obtained in Singh e Heldman (1993) were used, considering its respective mass fraction, as it follows,

$$\rho = (1 - \epsilon) / \sum (x_j / \rho_j), \quad (1)$$

$$Cp = \sum (x_j \times Cp_j), \quad (2)$$

$$k = 0.5 \times (\sum x_{vj} \times k_j + (1 / \sum (x_{vj} / k_j))), \quad (3)$$

$$x_{vj} = ((x_j / \rho_j) / (\sum (x_j / \rho_j))), \quad (4)$$

where  $\rho$  is density [ $\text{kg/m}^3$ ],  $x$  is each pure component mass fraction,  $C_p$  is specific heat [ $\text{J/kg}^\circ\text{C}$ ],  $x_{vj}$  is each pure component volumetric fraction and  $k$  is thermal conductivity [ $\text{W/m}^\circ\text{C}$ ].

Thermal diffusivity, by its turn, was calculated by  $\alpha = k/(\rho \times C_p)$  [ $\text{m}^2/\text{s}$ ]. These properties values in function of drying time are showed at Fig.3, where it can be observed that density increases with time, while specific heat, thermal conductivity and thermal diffusivity decrease with time. Density increases with time because the okara solids present a larger density than water's. However, the okara solid fraction has specific heat, thermal conductivity and thermal diffusivity smaller than water's. This means that as the water is removed of the product, heat transfer gets more difficult.

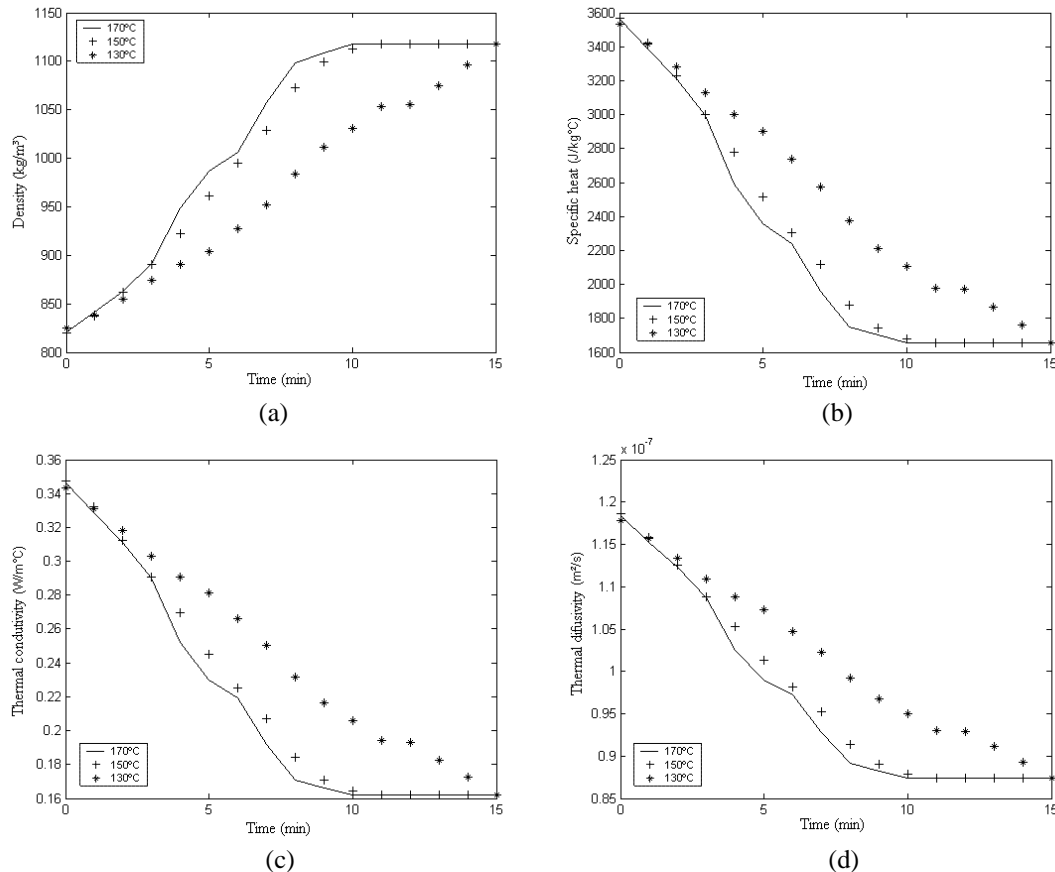


Figure 3 – Okara thermal properties versus process time (a) Density, (b) Specific heat, (c) Thermal conductivity and (d) Thermal diffusivity.

Convection heat transfer coefficient,  $h$  [ $\text{W/m}^2\text{C}$ ], was calculated by  $h = (Nu \times k)/d$ , where  $Nu$  is Nusselt number and  $k$  is air thermal conductivity [ $\text{W/m}^\circ\text{C}$ ]. In order to obtain  $Nu$  value, an empiric correlation between it and Reynolds number,  $Re$ , was used, which applies to the air flowing on spheres, that is  $Nu = 0.37Re^{0.6}$ . Reynolds number, by its turn, is obtained by  $Re = (\rho \times v \times d)/\mu$ , where  $\rho$  is air density [ $\text{kg/m}^3$ ],  $v$  is air velocity [ $\text{m/s}$ ],  $d$  is pellets diameter [ $\text{m}$ ] and  $\mu$  is air viscosity [ $\text{kg/m.s}$ ] (Incropera and Dewitt, 1990). The result for air velocity,  $Re$  and  $Nu$  at all drying temperatures tested are in Tab. 1.

Mass transfer coefficient,  $h_m$  [ $\text{kg/m}^2\text{s}$ ], was calculated as according to (Holman, 1996) by  $h_m = h / (\rho \times C_{p_a} \times (\alpha / D_m)^{2/3})$ , where  $C_{p_a}$  is air specific heat [ $\text{J/kg}^\circ\text{C}$ ],  $\alpha$  is air thermal diffusivity [ $\text{m}^2/\text{s}$ ],  $\mu$  is air viscosity [ $\text{kg/m.s}$ ] and  $D_m$  is water mass diffusivity in the air [ $\text{m}^2/\text{s}$ ]. The water apparent diffusivity ( $D_{ap}$ ) in okara for each process condition, after calculated all the former parameters, was obtained by the inverse problem employing Differential Evolution Optimization method (Storn and Price, 1995; Storn, 1997), using a computational code at Matlab. For this, the numerical simulations were made with an estimated interval for mass diffusivity of  $10^{-9}$  to  $10^{-11}$   $\text{m}^2/\text{s}$  and the best value inside this interval was obtained in combination with the other drying parameters.

The equilibrium humidity,  $X_e$ , was also obtained for each drying condition used.  $X_e$  was obtained using a correlation for okara between  $X_e$  and air relative humidity ( $UR$ ), as according to Lescano (2007), by  $X_e = ((m \times K \times UR) / (1 - K \times UR)) \times ((1 - q \times (1 - w) \times UR) / (1 - q \times UR))$ , where  $X_e$  is the equilibrium humidity dry basis [ $\text{kg/kg}$ ],  $m$ ,  $K$ ,  $q$  and  $w$  are fixed parameters for okara, which values are respectively 0.977, 0.148, 1.833 and 0.474, and  $UR$  is the air relative humidity [%] obtained experimentally as already mentioned at section 2.1. The results for  $X_e$ ,  $h$ ,  $h_m$  and  $D_{ap}$  for the different drying temperatures tested experimentally are found in Tab. 1.

Table 1 – Okara drying parameters obtained at different temperatures.

Temperature (°C)	$v$ (m/s)	$Re$	$Nu$	$X_e$ d.b. (kg/kg)	$h$ (W/m <sup>2</sup> °C)	$h_m \times 10^5$ (kg/m <sup>2</sup> s)	$D_{ap} \times 10^9$ (m <sup>2</sup> /s)
130	0.044	8.320	1.319	0.0078	8.93	1.26	4.1
150	0.051	9.279	1.408	0.0059	9.97	1.50	6.2
170	0.073	11.874	1.633	0.0032	11.72	1.63	7.4

As it can be seen above, apparent mass diffusivity ( $D_{ap}$ ) increases with temperature. Between the temperature values used,  $D_{ap}$  is the same of order of largeness expected for okara or foods with similar compositions, placing between  $10^{-9}$  and  $10^{-11}$  m<sup>2</sup>/s.

### 3 NUMERICAL MODELLING

The okara pellet computational domain can be approximated by a sphere. The geometry considered is one-dimensional at the coordinate spherical system, as illustrated at Fig. 4, and mass and heat transfer will be considered at radial sense.

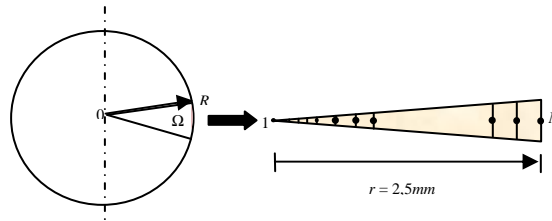


Figure 4 - Computational domain.

The drying phenomenon is governed by the heat and mass transfer. The former is represented by Fourier's Law and the second one by Fick's Law, Eqs. (5) and (6), respectively. To an one-dimensional system at spherical coordinates,  $r \in [0, R]$ , and in a spatial domain,  $\Omega$ , these equations are:

$$\frac{\partial T}{\partial t} = \frac{\alpha}{r^2} \left[ \frac{\partial}{\partial r} \left( r^2 \frac{\partial T}{\partial r} \right) \right], \quad (5)$$

$$\frac{\partial X}{\partial t} = \frac{1}{r^2} \left[ \frac{\partial}{\partial r} \left( r^2 D_{ap} \frac{\partial X}{\partial r} \right) \right], \quad (6)$$

where  $T$  is temperature [°C],  $r$  is the space coordinate [m],  $X$  is humidity content dry basis [kg/kg],  $\alpha$  is thermal diffusivity [W/m<sup>2</sup>°C], which varies with temperature at each interval of time, and  $D_{ap}$  is water apparent mass diffusivity [kg/m<sup>2</sup>°C] inside okara.

For heat transfer, boundary conditions are null heat flux at the center of the product and convective condition at its surface, as it follows,

$$\left. \frac{\partial T}{\partial r} \right|_{r=0} = 0, \quad (7)$$

$$-k \left. \frac{\partial T}{\partial r} \right|_{r=R} = h(T_R - T_{inf}) + \rho_s \Delta r \frac{\partial \bar{X}}{\partial t} [h_{fg} + c_v(T_R - T_{inf})], \quad (8)$$

where  $T_R$  is the last nodal point temperature [°C],  $T_{inf}$  is drying temperature [°C],  $\rho_s$  is okara solid fraction density [kg/m<sup>3</sup>],  $\bar{X}$  is the medium humidity dry basis along the section [kg/kg],  $h_{fg}$  is water vaporization latent heat [J/kg] and  $c_v$  is water vapor specific heat [J/kg°C]. The initial condition is  $T(r, t) = T_0$  at  $t = t_0$ ,  $r \in [0, R]$ , where  $T_0$  is the known temperature at the initial point obtained by experimental measurement [°C],  $t_0$  is process initial time [s] and  $R$  is okara pellet radius [m].

For the mass transfer, boundary conditions are null heat flux at the symmetry region and convective condition at the air-product interface, as it follows,

$$\left. \frac{\partial X}{\partial r} \right|_{r=0} = 0 \text{ at } r = 0, t \geq 0, \quad (9)$$

$$D_{ap} \frac{\partial X}{\partial r} \Big|_{r=R} = h_m (X_e - X_R) \quad (10)$$

where  $X_e$  is equilibrium humidity dry basis [kg/kg] and  $X_R$  is humidity dry basis at the okara pellet surface [kg/kg]. The initial condition is  $X(r, t) = X_0$  at  $t = t_0$ ,  $r \in [0, R]$ , where  $X_0$  is the known humidity at the initial point obtained by experimental measurement [ $^{\circ}\text{C}$ ],  $t_0$  is process initial time [s] and  $R$  is okara pellet radius [m].

Partial differential equations, Eqs. 5 to 10, were solved using the implicit finite difference method. The temporal and spatial discretizations were implemented in Matlab with the boundary and initial conditions.

### 3.1 Study of the process parameters

In a food drying process, it is desired to reduce the product humidity in order to increase its life time without causing darkening on it. The darkening reaction that happens at okara is Maillard reaction. Temperature has important influence on Maillard reaction velocity, mainly when temperatures are higher than  $120^{\circ}\text{C}$ , where the temperature increase enlarges the reaction velocity on 2 to 3 times for each  $10^{\circ}\text{C}$  increment (Araújo, 2004).

In order to compare the color of the products dried at different process temperatures, a control sample, which was not dried, was used. At Fig. 5 it can be seen that the non-dried pellets present a light color. Also at the Fig. 5 it is observed that when dried the pellets acquire a golden color and as the temperature increases, the product darkening increases either. The okara pellets dried at  $130^{\circ}\text{C}$  (for 15 minutes) presents a relatively light color, however the sample dried at  $150^{\circ}\text{C}$  (for 10 minutes) presents an undesirable darkening level, while the product submitted to the drying at  $170^{\circ}\text{C}$  (for 9 minutes) presents a burned color, showing exaggerated darkening.

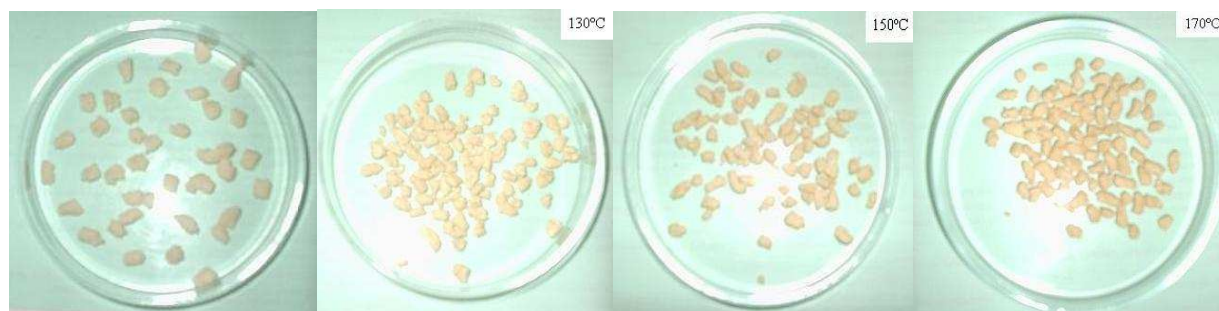


Figure 5 – Non-dried pellets and pellets dried at different temperatures.

### 3.2. Comparison between numerical and experimental results

Three drying processes were simulated numerically and for each process the humidity and temperature profiles versus time were obtained. For the drying processes at  $130^{\circ}\text{C}$ ,  $150^{\circ}\text{C}$  and  $170^{\circ}\text{C}$ , the correlation coefficients ( $R^2$ ) obtained from the comparison between experimental and numerical results for temperature were 0.9963, 0.9944 and 0.9982, respectively, and the  $R^2$  for humidity were 0.9973, 0.9994 and 0.9995, respectively. At Figs. 6-8 are shown the results obtained by numerical simulations.

In the drying process at  $130^{\circ}\text{C}$ , the humidity experimental values between fifth and ninth minutes of process are higher than the numerical ones, but the concordance is still adequate, as it can be seen at Fig. 6. For temperature, by its turn, the experimental values at this same time interval are lower than the simulated ones. However, it is considered that experimental and numerical results are in agreement. In the process at  $150^{\circ}\text{C}$ , it can be seen that there are differences at the last drying minutes for the humidity profile, as shows Fig. 7a. According to the numerical results, drying would last a few minutes more to obtain the desired final humidity. Though, for temperature, experimental values have good concordance with numerical values. The process at  $170^{\circ}\text{C}$  presents a satisfactory agreement between experimental and numerical data, however at Fig. 8 it can be seen that humidity in the final of the process is again lower than the experimental results.

From the observation of Figs. 6-8, it can be noticed that the simulations present satisfactory results, with  $R^2$  values higher than 0.99. A tendency for almost all processes was the slight difference for humidity at the last minutes of process. Probably the numerical value is more reliable, because the equilibrium humidity for each drying temperature is around  $0.01\text{kg/kg}$  d.b. (about 1% wet basis), avoiding that the product humidity reaches zero, as it happened experimentally.

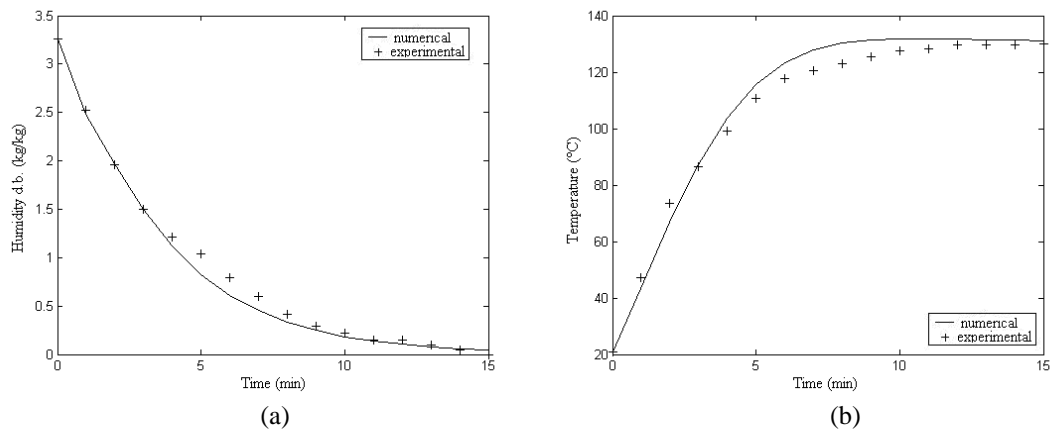


Figure 6 – Numerical and experimental results during the drying process at 130°C for the (a) humidity and (b) temperature profiles, in function of time.

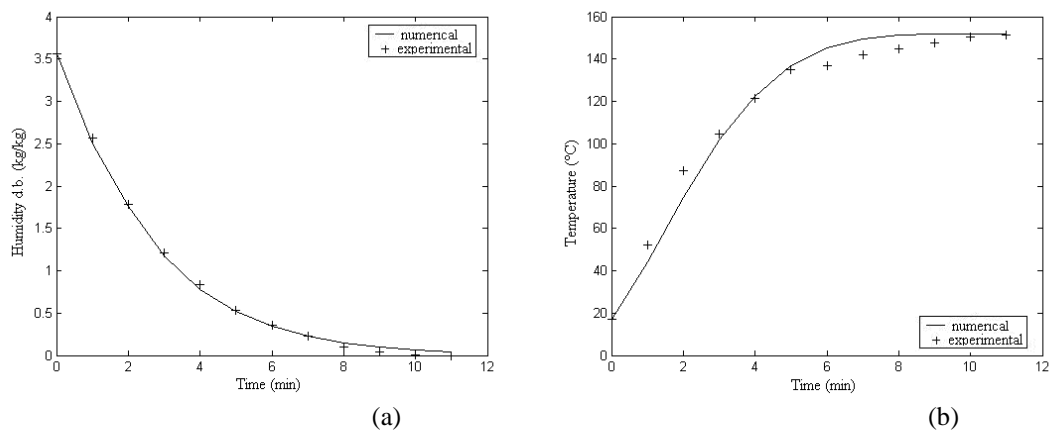


Figure 7 – Numerical and experimental results during the drying process at 150°C for the (a) humidity and (b) temperature profiles, in function of time.

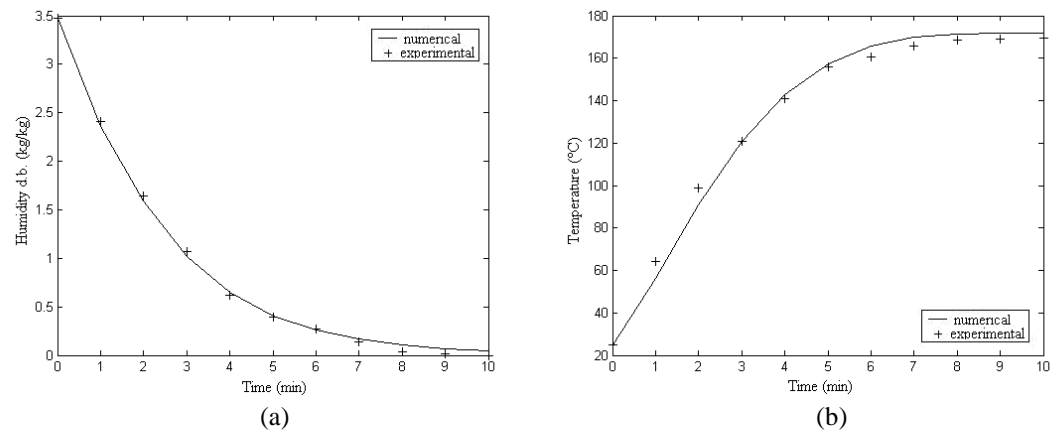


Figure 8 – Numerical and experimental results during the drying process at 170°C for the (a) humidity and (b) temperature profiles, in function of time.

#### 4. CONCLUSIONS

In this work, the main motivation was to contribute for the profit of okara, a high nutritive value product, which has been discarded and generated high expenses with effluent treatment in the tofu and soy beverage industries, by a drying process. It was concluded that the proposed drying method, that is, the 5 mm okara pellets drying in a fixed bed dryer, is efficient to obtaining dried okara with good process velocity and good formatting of the final product. In respect with the dried pellets' color, the 130°C temperature offers the better results, as expected. It is known that Maillard reaction velocity depends on temperature, hence, in order to decrease drying time obtaining reduced darkening levels, it is enough to use a drier that provides higher air velocities, because the range of velocities used experimentally in this work (in function of the air supply used) is very limited (0.044 to 0.073 m/s). About the mathematical modeling

developed here to describe the heat and mass transfer phenomenon during the okara (in the shape of spheres) drying based on the finite difference method, it was concluded that it is possible to obtain information about drying processes without the need of experimental tests for each set of process conditions used, being enough to have the product composition, which can be found at specialized literature or can be made at laboratory. The comparison between experimental and numerical results was satisfactory, with  $R^2$  values higher than 0.99. Thus, it is considered that the present work has attained its goals, contributing scientifically to the food drying process simulation theme and complementing the works already existent about okara drying.

## ACKNOWLEDGEMENTS

Camila Augusto Perussello thanks CAPES for the master scholarship received between 2006 and 2008.

## 5. REFERENCES

- Araújo, J. M. A. (2004). "Química de alimentos: teoria e prática". 3. ed. Viçosa: Ed. UFV, 478 p.
- Coronel, E. L.; Tobinaga, S. (2004). "Drying the okara in a spouted bed". Proceedings of the 14th International Drying Symposium. p.1-5.
- Incropera, F. P.; Dewitt, D. P. (1990). "Fundamentals of heat and mass transfer". 3 rd ed. New York: J. Wiley & Sons, 919p.
- Lescano, A. A.; Tobinaga, S. (2004). "Modelo codificado e real para a difusividade efetiva da secagem do resíduo do extrato hidrossolúvel de soja". Revista Brasileira de Produtos Agroindustriais, V.6 (1), p.17-25.
- Lescano, A. A.; Fraile N.; V., Rocha, S. C. S. (2005). "Drying of the soymilk residue "okara" in spouted bed". 2nd Mercosur Congress on Chemical Engineering e 4th Mercosur Congress on Process Systems Engineering, p.1-10.
- Lescano, A. A.; Fraile Neto, V.; Rocha, S. C. S. (2007). "Higroscopicidade do resíduo de leite de soja (okara) seco em leite de jorro com inertes". XXXIII Encontro Brasileiro de Sistemas Particulados, p.1.
- Mannaperuma, J. D.; Singh, R. P. (1988). "Prediction of freezing and thawing times of foods using a numerical method based on enthalpy". Journal of Food Science, V.53 (2), p. 626-630.
- Singh, P. R.; Heldman, N, D. R. (1993). "Introduction to food engineering". 2. ed. USA: Editora Acadêmica, 499p.
- Storn, R. and Price, K., 1995. "Differential evolution: a simple and efficient adaptive scheme for global optimization over continuous spaces", Technical Report TR-95-012, International Computer Science Institute, Berkeley, CA, USA.
- Storn, R., 1997. "Differential evolution - a simple and efficient heuristic for global optimization over continuous spaces". Journal of Global Optimization, 11, p.341-359.
- Taruna, I.; Jindal, V. K. (2002). "Drying of soy pulp (okara) in a bed of inert particles". Drying Technology, V.20(4&5), p.1035-1051.
- Tarsumi, E.; Li, F. D.; Li, L. T.; Sun, J. F. (2006). "Effect of electrohydrodynamic (EHD) technique on drying process and appearance of okara cake". Journal of Food Engineering, V.77, p. 275-280.

## RESPONSIBILITY NOTICE

The authors Camila Augusto Perussello, Viviana Cocco Mariani and Álvaro César Camargo do Amarante are the only responsible for the printed material included in this paper.